

The Effect of Excess Y_2O_3 Addition on the Mechanical Properties of Melt-Processed YBCO Superconductor

Alev Aydiner · Bakiye Çakır · Mehmet Başoğlu · Ekrem Yanmaz

Received: 4 December 2009 / Accepted: 2 June 2010 / Published online: 16 June 2010
© Springer Science+Business Media, LLC 2010

Abstract In this study, two kinds of melt-processed YBCO samples with Y_2O_3 addition were fabricated and their microstructures were defined by XRD analysis and polarized light optical microscopy. The mechanical properties of these compounds have been investigated by measuring the Vickers hardness. The superconducting transition temperature was determined by inductive measurements for oxygenated and non-oxygenated samples. The compacted powders were located on a crucible with a buffer layer of Y_2O_3 and a crucible with Y_2O_3 powder freely poured to avoid liquid to spread on the furnace plate. It was found that the sample located on crucible with freely poured Y_2O_3 powder has shown almost single crystal and indicated a very sharp transition curve.

Keywords YBCO · Single crystal · MPMG method · Excess Y_2O_3 addition

1 Introduction

Melt-textured $YBa_2Cu_3O_y$ (YBCO) is suitable for many applications such as magnetic bearings, flywheel energy storage systems, non-contact transport devices and levitation and trapped-field magnets [1, 2]. The control of the growth

process conditions is essential in order to create homogeneous, monolithic samples with a large number of intrinsic flux pinning centers. Therefore many kinds of modified melt processes have been developed, such as melt texture growth (MTG), liquid phase processing (LPP), quench and melt growth (QMG), melt powder melt growth (MPMG), powder melting process (PMP) and flame quench melt growth (FQMG) [3–5].

In addition, in order to answer the technological requests, research groups have concentrated their attention on the study of the mechanical properties of melt-textured YBCO superconductors [6–10]. These studies have reported on the hardness, Young's modulus and yield strength of YBCO compounds.

The oxygen content of the bulk and thin film YBCO is a very important parameter related to its superconducting properties [11, 12]. In addition, it is known that Y_2O_3 layer on a substrate has effect on the growth of $YBa_2Cu_3O_{7-y}$ thin film [13], because the YBCO thin film on that layer is *c*-axis oriented and shows good in-plane alignment. The Y_2O_3 buffer layer on crucible also prevents the liquid to spread on the furnace plate during the crystal growth of YBCO [14]. For this reason, in this study, the effect of oxygenation and Y_2O_3 layer on the melt growth process was investigated and the effect on the mechanical properties was described.

2 Experimental Procedure

Appropriate amounts of Y_2O_3 , $BaCO_3$ and CuO powders in stoichiometric ratio of 1:2:3 were mixed by a mortar machine for 1 h to get a homogeneous mixture. Mixture placed in an alumina crucible after milling process was put into muffle furnace for calcination process. The powders were

A. Aydiner (✉) · M. Başoğlu · E. Yanmaz
Physics Department, Karadeniz Technical University,
61080 Trabzon, Turkey
e-mail: alevaydiner@gmail.com

B. Çakır
Physics Department, Artvin Çoruh University, 08000 Artvin,
Turkey

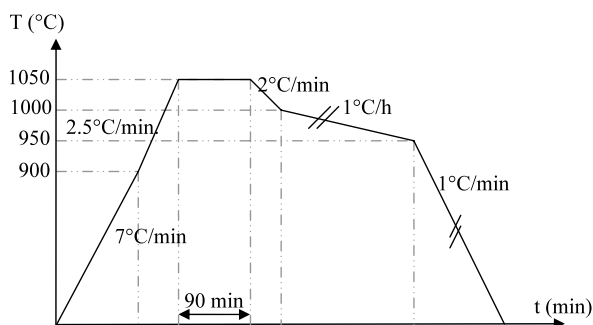


Fig. 1 Schematic diagram of thermal process for YBCO samples

held at 900°C for 30 hours in air atmosphere. After first 15 hours, the crucible was removed from the furnace and cooled in air to the room temperature. For increasing homogeneity of a bulk-like sample, an intermediate grinding was performed throughout for 15 minutes and then it was placed back into the furnace. At the end of the calcination process, the black powders were ground again for 1 hour to obtain a more homogeneous mixture. The fine powders were then placed into a platinum crucible and put into the muffle furnace at room temperature. The furnace temperature was increased to 1450°C and held at that temperature for 5 min. to get molten material. The molten material was then poured onto a copper plate, and afterwards sandwiched with another copper plate to protect phase condition during melt. The obtained thin platelets were ground again for 1 hour to achieve fine powder. Differential thermal analysis (DTA) was performed on the calcined powder to determine its peritectic decomposition temperature on heating.

The precursor powder weighted 4 g was pressed into a pellet 13 mm in diameter under 300 MPa pressure and held for 1 minute at that pressure. In this study, two kinds of melt-processed YBCO samples (Y1050 and Y1050*) were fabricated for a growth temperature of 1050 °C. While the sample Y1050 was located on a crucible with a buffer layer of Y_2O_3 , the sample Y1050* was located on a crucible with a buffer layer of freely poured Y_2O_3 powder. The schematic diagram of thermal process of these samples was given in Fig. 1. Finally, the grown samples were annealed at 500°C for 24 h in flowing oxygen and then cooled to room temperature at a rate of $1^\circ C \text{ min}^{-1}$ in oxygen.

X-ray diffraction data were collected by using a Rigaku D/Max III C diffractometer, employing $CuK\alpha$ ($\lambda = 1.5418 \text{ \AA}$, 40 kV, 30 mA) radiation. 2θ range 20 to 60° was scanned in steps of 0.02° with a counting time 3°/min. The optical micrographs were taken using a polarized light microscope. The superconducting transition temperature (T_c) was determined by inductive measurements for oxygenated and non-oxygenated samples.

Hardness measurements of the oxygenated samples were performed on the polished surface of the examined samples

with a digital micro hardness tester (Struers Duramin-3) at room temperature. A Vickers pyramidal indenter with different loads (0.981 N, 1.960 N, 2.940 N, 4.910 N and 9.810 N) was applied, for 10 s for all trials, and the diagonals of indentation were measured with an accuracy of $\pm 0.1 \mu\text{m}$. Indentations were made at different surface parts of the samples in such a way that the distance between any two indentations was no less than two times the diagonal of the indentation mark to avoid surface effects due to neighboring indentation. An average of 5 readings at different locations on the specimen surfaces was taken to obtain reasonable mean values for each load.

The room temperature Vickers micro hardness was estimated according to the following (1) [6]:

$$H_v = 1854.4(F/d^2) \text{ (GPa)} \quad (1)$$

where F is the contact load (in N) and d is the diagonal length of the indentation mark (in μm).

In most materials, the elastic modulus (Young's modulus) “ E ” is related to the bulk hardness “ H_v ” by (2) [15, 16]:

$$E = 81.9635H_v \quad (2)$$

In addition, yield strength Y is related to the hardness by (3) [17, 18]:

$$Y \approx \frac{H_v}{3} \quad (3)$$

The bulk density of the samples was determined by the Archimedes method using diethyl phthalate as the immersion liquid.

3 Results and Discussion

Figure 2 shows XRD pattern of Y1050* and Y1050 samples. Y1050* and Y1050 means that the sample located on crucible with freely poured Y_2O_3 and buffer layer of Y_2O_3 powder, respectively. When we look with naked eye onto surface of samples, a very big crystal (8 mm diameter) and another two small crystals, which can be neglected comparing with big crystal, were observed for Y1050*. It was observed that the crystals of sample Y1050 were smaller and more granular than Y1050*. It can be expected that Bragg reflections will be very hard to see using powder diffractometer which was not single crystal diffractometer. For taking reflection, the sample direction was changed with a certain angle inside the sample holder until we got Bragg reflection. But there were no clear differences in the pattern of the big grained Y1050* sample. It can be seen in Fig. 2(b) that the standard peak of the Y123 sample ($2\theta = 32.75^\circ$) was observed with 7000 cps intensity for Y1050. The conclusion shows that the whole pellet behaves as a single crystal.

Fig. 2 XRD patterns of samples (a) Y1050* and (b) Y1050

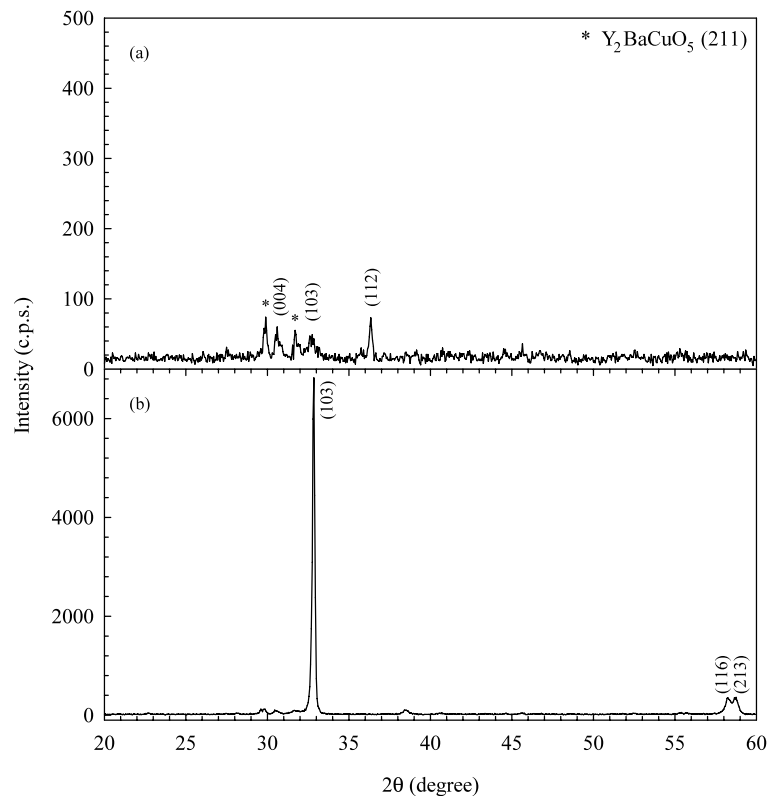


Figure 3 indicates polarized light optical micrographs of Y1050* and Y1050. It can be seen on both two micrographs that the connectivity of grains is very good and clear. Besides, it was observed that secondary non-superconducting phases not joined in the reaction were not gathered through the grain boundaries and distributed homogeneously into the grains during the crystal growth process. It was predicted from these micrographs that the critical current density would be high. Longitudinal cracks perpendicular to the crystal growth direction were observed for all samples, as reported before [19]. To minimize these cracks, a wide range of 211 non-superconducting phases distributed homogeneously into the 123 main structures are needed. Also, it is known that cracks limit the current carrying capacity of the superconductor [19].

The variations of micro hardness of the samples are plotted as a function of applied load in Fig. 4. It is shown that the micro-hardness values decrease rapidly with increasing load in a range up to a load of 4.910 N and then decrease in a narrow interval for higher loads. This was also observed for bulk Y-123 prepared by the conventional melt-textured growth (MTG) method and vertical gradient freeze (VGF) methods [6]. It is also observed that the variation of the micro hardness with load has a similar shape for Y1050 and Y1050* samples, although the numerical values are different. The hardness values are in good agreement with those obtained by other groups for the YBCO system. This is be-

cause the bulk hardness of YBCO determined at room temperature has been mostly obtained by conventional Vickers measurements and the values are in the range from 5 to 10 GPa [7, 10].

The calculated load dependent Vickers hardness (H_v), elastic modulus (E) and yield strength (Y) by using (1)–(3) for different applied loads are summarized in Table 1. This table reveals that the increase of H_v and E values of both samples with increasing density may be attributed to a decrease in the grain size. The decrease in grain size suppresses the cracking tendency. Saleh [16] and Goretta [20] found that the Young's modulus increases with an increase in density, as usually observed for a great number of structural ceramics. On the other hand the differences between the densities of Y1050 and Y1050* samples are not explicitly defined.

Figure 5 shows the temperature dependence of the inductance as a function of temperature for oxygenated and non-oxygenated Y1050* and Y1050 samples. While onset $T_c = 94$ K, with 6 K transition width, was obtained for the non-oxygenated Y1050 sample, the oxygenated Y1050 sample showed a sharp superconductive transition. However, sample Y1050* showed a sharp superconducting transition for both non-oxygenated and oxygenated conditions. As shown in Fig. 5, the effect of oxygenation process is much more pronounced for Y1050 than Y1050*. Because Y1050* was almost single crystal (8 mm diameter), the ap-

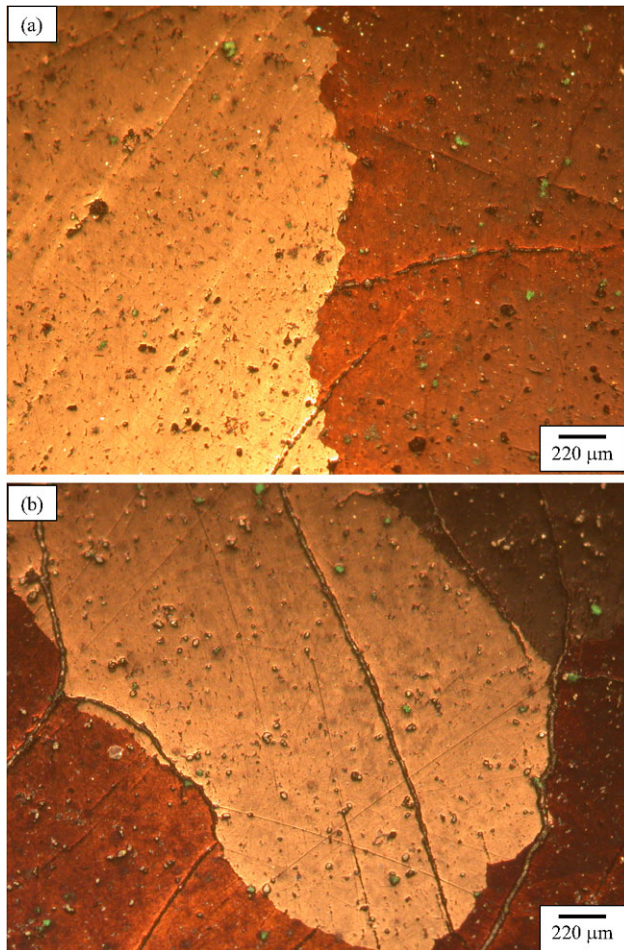


Fig. 3 Polarized light optical micrographs of samples (a) Y1050* and (b) Y1050

plied oxygenation of 24 h duration is insufficient. It is known that approximately 200 h oxygenation duration is required for YBCO single crystals [11].

4 Conclusion

1. The sample located on to crucible with freely poured Y_2O_3 showed better microstructure and superconducting properties.
2. The micro-hardness values decrease rapidly with increasing load up to 4.910 N and then decrease in a narrow interval for higher loads.
3. Bulk hardness of YBCO samples determined at room temperature has been obtained by conventional Vickers

Table 1 The load dependence of microscopic mechanical properties: Vickers hardness (H_v), elastic modulus (E) and yield strength (Y) for Y150 and Y1050* samples

Sample	d (g/cm ³)	F (N)	H_v (GPa)	E (GPa)	Y (GPa)
Y1050	5.929	0.981	10.649	872.829	3.550
		1.960	9.284	760.949	3.095
		2.940	8.245	675.789	2.748
		4.910	7.463	611.694	2.488
		9.810	6.157	504.649	2.052
Y1050*	5.897	0.981	9.574	784.719	3.191
		1.960	8.355	684.805	2.785
		2.940	7.680	629.480	2.560
		4.910	7.026	575.876	2.342
		9.810	5.543	454.324	1.848

Fig. 4 Load dependence of hardness for Y150 and Y1050* samples

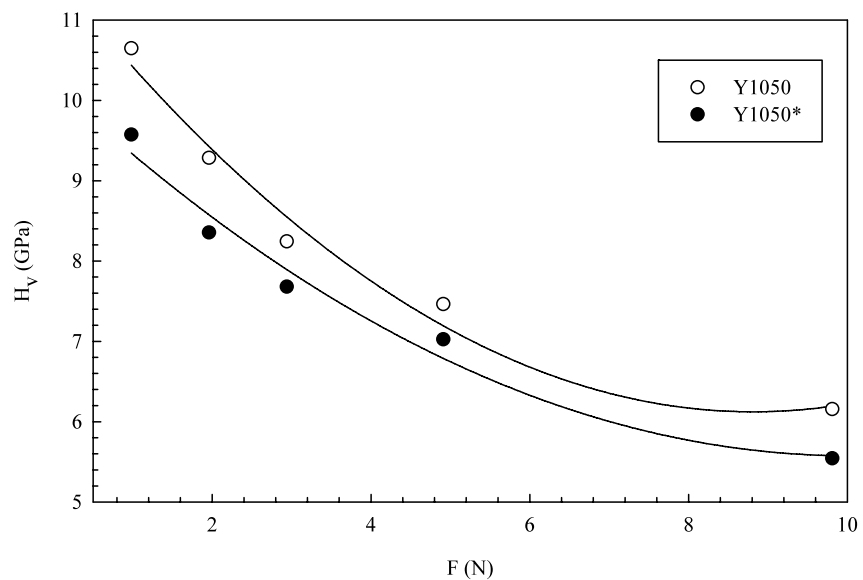
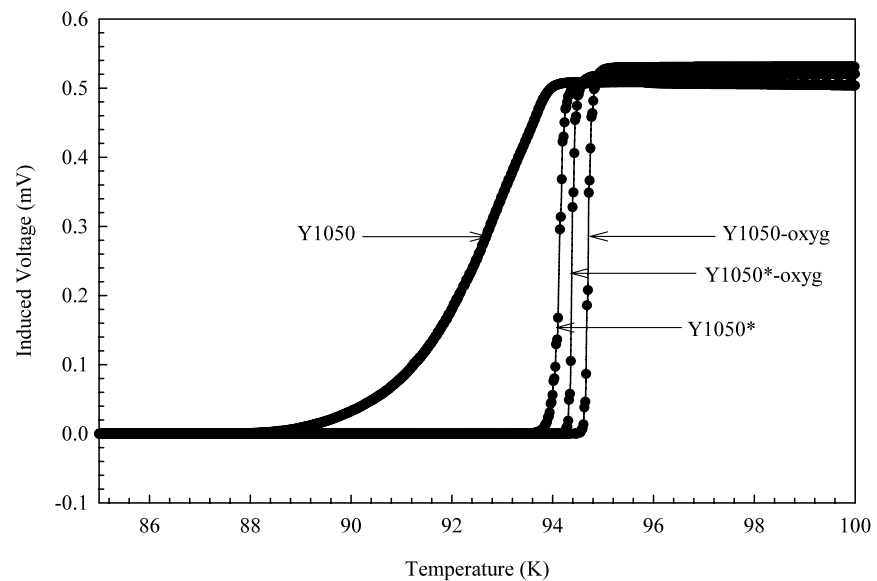


Fig. 5 Inductive T_c measurement for non-oxygenated and oxygenated Y1050* and Y1050 samples



measurements and the values are in the range from 5 to 10 GPa at various loads.

- The oxygenation is a very effective way to increase the transition temperature of samples for the YBCO family.

Acknowledgements This study was supported by Turkish Scientific and Research Council (TUBITAK) research grant (TBAG-107T751) and Karadeniz Technical University research grant (BAP-2008.111.001.8). The authors would like to thank Dr. Gençğa Pürçek for his contribution during discussion of the hardness results and Ph.D. student Onur Saray for help in measuring of Vickers micro hardness in the Mechanical Engineering Department of Karadeniz Technical University.

References

- Murakami, M.: *Physica C* **357–360**, 751 (2001)
- Hull, J.R.: *Supercond. Sci. Technol.* **13**, R1–R15 (2000)
- Feng, J., Lu, Y., Zhang, L.P., Xu, X., Chen, S., Zhang, C., Xiong, X., Liu, G.: *Physica C* **59**, 52–55 (2007)
- Murakami, M.: *Supercond. Sci. Technol.* **5**, 185–203 (1992)
- Ateş, A., Yanmaz, E.: *J. Alloys Comp.* **279**, 220–228 (1998)
- Leenders, A., Ullrich, M., Freyhardt, H.C.: *Physica C* **279**, 173–180 (1997)
- Lubenets, S.V., Natsik, V.D., Fomenko, L.S., Kaufmann, H.-J., Bobrov, V.S., Izotov, A.N.: *Fiz. Niz. Temp.* **23**(8), 902–908 (1997)
- Yoshino, Y., Iwabuchi, A., Noto, K., Sakai, N., Murakami, M.: *Physica C* **357–360**, 796–798 (2001)
- Mathieu, J.P., Cano, I.G., Koutzarova, T., Rulmont, A., Vanderbenden, Ph., Dew-Hughes, D., Ausloos, M., Cloots, R.: *Supercond. Sci. Technol.* **17**, 169–174 (2004)
- Foerster, C.E., Lima, E., Rodrigues, Jr., P., Serbana, F.C., Lepienski, C.M., Cantão, M.P., Jurelo, A.R., Obradors, X.: *Braz. J. Phys.* **38**, 341–345 (2008)
- Zheng, M.H., Xiao, L., Ren, H.T., Jiao, Y.L., Chen, Y.X.: *Physica C* **386**, 258–261 (2003)
- Diko, P., Chaud, X., Antall, V., Kánuchová, M., Šefčíková, M., Kováči, J.: *Supercond. Sci. Technol.* **21**, 115008–115010 (2008)
- Hasegawa, M., Yoshida, Y., Iwata, M., Ishizawa, K., Takai, Y., Hirabayashi, I.: *Physica C* **336**, 295–299 (2000)
- Chaud, X., Isfort, D., Beaugnon, E., Tournier, R.: *Physica C* **341–348**, 2413–2416 (2000)
- Khalil, S.M.: *Physica B* **391**, 130–135 (2007)
- Saleh, S.A., Khalil, S.M., Ibrahim, E.M.M.: *Supercond. Sci. Technol.* **20**, 372–376 (2007)
- Aydın, H., Cakiroglu, O., Nursoy, M., Terzioglu, C.: *Chin. J. Phys.* **47**(2), 192–206 (2009)
- Khalil, S.M.: *J. Phys. Chem. Solids* **62**, 457–466 (2001)
- Murakami, M.: *Mod. Phys. Lett. B* **4**, 163–179 (1990)
- Goretta, K.C., Kullberg, M.L., Bärt, D., Risch, G.A., Routbort, J.L.: *Supercond. Sci. Technol.* **4**, 544–547 (1991)

Copyright of Journal of Superconductivity & Novel Magnetism is the property of Springer Science & Business Media B.V. and its content may not be copied or emailed to multiple sites or posted to a listserv without the copyright holder's express written permission. However, users may print, download, or email articles for individual use.